

This is a self-archived version of an original article. This version may differ from the original in pagination and typographic details.

Author(s): Kumar, Parveen; Komulainen, Joonas; Frontera, Antonio; Ward, Jas S.; Schalley, Christoph; Rissanen, Kari; Puttreddy, Rakesh

Title: Linear bis-Coordinate Silver(I) and Iodine(I) Complexes with R₃R₂R₁N Tertiary Amines

Year: 2023

Version: Published version

Copyright: © 2023 the Authors

Rights: CC BY 4.0

Rights url: <https://creativecommons.org/licenses/by/4.0/>

Please cite the original version:

Kumar, P., Komulainen, J., Frontera, A., Ward, J. S., Schalley, C., Rissanen, K., & Puttreddy, R. (2023). Linear bis-Coordinate Silver(I) and Iodine(I) Complexes with R₃R₂R₁N Tertiary Amines. *Chemistry : A European Journal*, 29(69), Article e202302162. <https://doi.org/10.1002/chem.202302162>

Hot Paper

Linear *bis*-Coordinate Silver(I) and Iodine(I) Complexes with $R_3R_2R_1N$ Tertiary AminesParveen Kumar,^[a] Joonas Komulainen,^[a] Antonio Frontera,^[b] Jas S. Ward,^[a] Christoph Schalley,^[c] Kari Rissanen,^{*[a]} and Rakesh Puttreddy^{*[a]}

Homoleptic $[L-I-L]^+$ iodine(I) complexes (where L is a $R_3R_2R_1N$ tertiary amine) were synthesized via the $[L-Ag-L]^+ \rightarrow [L-I-L]^+$ cation exchange reaction. In solution, the amines form $[R_3R_2R_1N-Ag-NR_1R_2R_3]^+$ silver(I) complexes, which crystallize out from solution as the *meso*- $[L-Ag-L]^+$ complexes, as characterized by X-ray crystallography. The subsequent $[L-I-L]^+$ iodine(I) analogues were extremely reactive and could not be isolated in the solid state. Density functional theory (DFT) calculations

were performed to study the Ag^+-N and I^+-N interaction energies in silver(I) and iodine(I) complexes, with the former ranging from -80 to -100 kJ mol^{-1} and latter from -260 to -279 kJ mol^{-1} . The X-ray crystal structures revealed $Ag^+ \cdots C_\alpha$ and $Ag^+ \cdots H-C$ short contacts between the silver(I) cation and flexible N-alkyl/N-aryl groups, which are the first of their kind in such precursor complexes.

Introduction

Chirality is a fundamental asymmetry property defined by the IUPAC^[1] as the geometry of a rigid object or spatial arrangement of atoms that is non-superposable with its respective mirror image. The chiral center of molecules and complexes can be any atom, such as carbon, nitrogen, phosphorous, or sulfur, having four different substituents that are spatially fixed.^[2–5] Tertiary amines with three different substituents are chiral when their lone pair is considered as the fourth substituent. Under normal conditions the nitrogen lone pair undergoes very fast umbrella-like inversion,^[6] rendering such tertiary amines effectively racemic and enantiomer separation impossible. In certain conditions the separation of the enantiomers has been accomplished, *viz.* when the lone pair inversion is slow due to the bicyclic scaffold (e.g., Sparteine^[7]) or in configurationally stable $R_3R_2R_1N^+$ ($R_1 \neq R_2 \neq R_3 \neq R_4$) quaternary ammonium cations.^[8] Besides organic chemistry methods that use covalent

bonds to synthesize configurationally stable tertiary amines,^[9] supramolecular approaches employ non-covalent bonds, such as hydrogen bonds,^[10–12] $C-H \cdots \pi$,^[13] and boron-nitrogen dative bonds,^[14] to control the nitrogen inversion.

For instance, hydrogen bonding is increasingly used to control the nitrogen inversion in aziridine complexes,^[15] which are configurationally dynamic and have been used as molecular switches.^[16] As chiral tertiary amine coordination complexes, the bidentate tertiary diamines and transition metal (M) complexes have received the most prominent attention, as the resulting M–L coordination bond(s) fix the nitrogen atom(s) into a specific tetrahedral configuration.^[17] Gagné et al. reported enantio- and diastereopure N-chiral palladium complexes, in which the amines are fixed into either a *dl* pair or a *meso* form and then employed in asymmetric catalysis (Figure 1).^[18]

Surprisingly, the linear *bis*-coordinate $[N-M-N]^+$ transition metal ($M = Ag$ or Au) complexes with $R_3R_2R_1N$ tertiary amines are extremely rare, especially as X-ray structures. Only one example, the *bis*-(9-(methylaminomethyl)anthracene)₂Ag]PF₆^[19] has been reported; it crystallizes in a centrosymmetric monoclinic space group $C2/c$ and is thus the *meso*-form. No optically pure *R,R/S,S* $[N-M-N]^+$ complexes with monodentate $R_3R_2R_1N$ tertiary amines have been reported.

The three-center-four-electron ($3c-4e$) $[N-X-N]^+$ halogen bonds in Barluenga-type halogen(I) complexes, like *bis*(pyridine)X⁺ ($X = Cl, Br, I$) have been shown to be partly electrostatic and covalent in nature with total binding ener-

[a] P. Kumar, J. Komulainen, Dr. J. S. Ward, Prof. Dr. K. Rissanen, Dr. R. Puttreddy
Department of chemistry
University of Jyväskylä
P.O. BOX 35, FI-40014, Jyväskylä (Finland)
E-mail: kari.t.rissanen@jyu.fi
rakesh.r.puttreddy@jyu.fi

[b] Prof. Dr. A. Frontera
Department of Chemistry
Universitat de les Illes Balears
Ctra de Valldemossa km 7.5, 07122 Palma de Mallorca (Balears) (Spain)

[c] Prof. Dr. C. Schalley
Institut für Chemie und Biochemie
Freie Universität Berlin
Arnimallee 20, 14195 Berlin (Germany)

Supporting information for this article is available on the WWW under <https://doi.org/10.1002/chem.202302162>

© 2023 The Authors. Chemistry - A European Journal published by Wiley-VCH GmbH. This is an open access article under the terms of the Creative Commons Attribution License, which permits use, distribution and reproduction in any medium, provided the original work is properly cited.

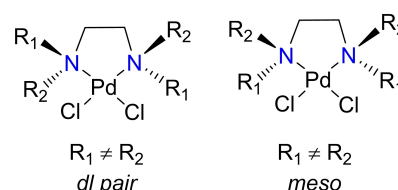


Figure 1. The *dl* pair and *meso* form of Pd-complexes of ethylenediamine derivative.^[20]

gies $> 160 \text{ kJ mol}^{-1}$ (for iodine(I) complexes).^[20] In these complexes, the halonium cation, X^+ , has $p_x^2 p_y^2 p_z^0$ configuration.^[21] The two lobes of p_z -orbital carry the positive charge and $[L-X-L]^+$ halogen bonds (XB) are created by charge transfer from the pyridinic nitrogen atoms to the vacant p_z -orbital.^[21] Tertiary amines, like quinuclidine,^[22] triethanolamine,^[23] DABCO,^[24] form similar $[L-X-L]^+$ halogen-bonded complexes.^[25] The application of halogen(I) complexes as reagents, mainly the $[(\text{pyridine})_2]^+$ species, have been investigated for oxidations,^[26] and C–I bond formations.^[27,28] In the last decade the studies on homoleptic $[L_1-I-L_2]^+$ (where $L_1=L_2$)^[20,29–32] and heteroleptic $[L_1-I-L_2]^+$ ($L_1 \neq L_2$)^[33–36] complexes have attracted more attention in supramolecular chemistry^[21] and have been successfully utilized in the synthesis of capsules,^[37–39] helicates,^[40] and metal-organic frameworks.^[41] These studies exclusively use $[N-I-N]^+$ motifs of either aromatic N-heterocycles (pyridine or imidazole derivatives) or bicyclic tertiary amines (quinuclidine^[22] and DABCO^[24]).

The chirality of the bidentate tertiary diamine-metal complexes has been established and consequently shown to be active in asymmetric catalysis.^[18] On the other hand, the known activity of the $[N-I-N]^+$ pyridine complexes as efficient iodination and oxidation reagents, raises a question if the spatial arrangement of the substituents in $R_3R_2R_1N$ amines could be fixed by the iodine(I) coordination, leading to chiral tertiary amine iodine(I) complexes, namely the R,R - and S,S -enantiomers, or to the *meso*-form of $[R_3R_2R_1N-I-NR_1R_2R_3]^+$ (Figure 2). This family of complexes would be appealing due to their unusual feature of chirality originating from the N-stereocenters when bonded to a reactive iodine(I) ion, which could offer new halogen(I)-based reagents or chiral supramolecular assemblies.

Results and Discussion

Herein, we report the successful synthesis of the iodine(I) complexes (**1b–6b**) from their silver(I) analogues (**1a–6a**) via the $[L-Ag-L]^+ \rightarrow [L-I-L]^+$ cation exchange reaction upon reaction with elemental iodine (Figure 3).^[20] The amines ($L=1-6$) used in this study are synthesized using a method previously described in the literature.^[42] The prepared trifluoroacetate salts (**1c–6c**) were used to identify the potential formation of the protonated ligand $[LH]^+$ during the $[L-Ag-L]^+ \rightarrow [L-I-L]^+$ cation exchange process. It is worth noting that the salts **1c–6c** have

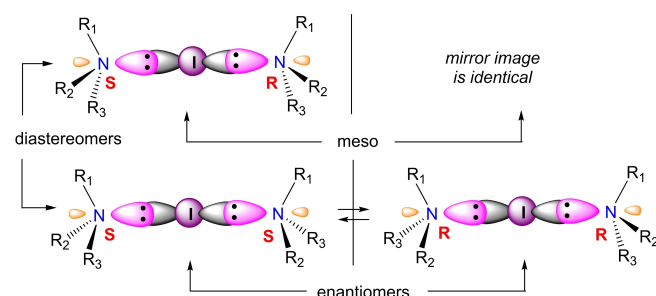


Figure 2. Schematic representation of R,R , S,S and *meso*-halogen(I) complexes when $R_1 \neq R_2 \neq R_3 = \text{alkyl/arylalkyl}$.

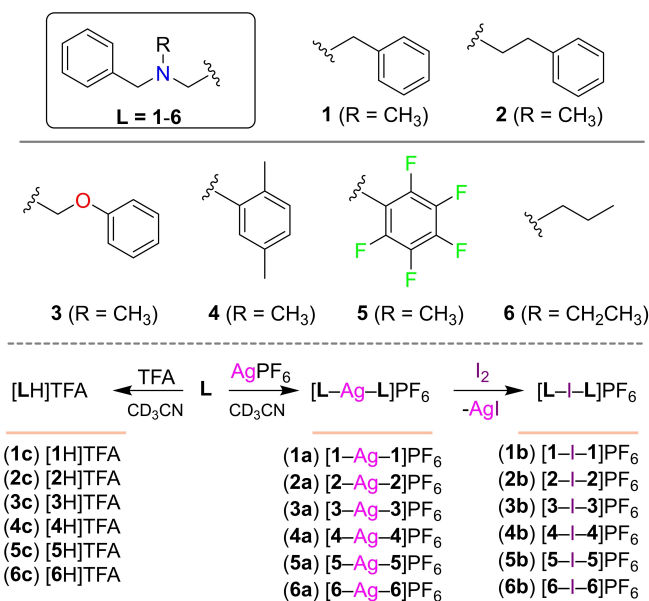


Figure 3. List of tertiary amine ligands, $L(1-6)$, and their $[L-Ag-L]PF_6$ (**1a–6a**) and $[L-I-L]PF_6$ (**1b–6b**), $[LH]CF_3COO$ (**1c–6c**) complexes.

four different substituents, with the hydrogen acting as the fourth unique substituent, are 1:1 mixtures or the R - and S -enantiomers, *viz.* racemic. The complexation of the tertiary amine ligands **1–6** into silver(I) and iodine(I) complexes is monitored by 1H and $^1H-^{15}N$ HMBC NMR spectroscopy. For comparison, triethylamine (**tea**) and diisopropylamine (**dipa**) were used as ligands, leading to $[\text{tea-Ag-tea}]PF_6$, $[\text{tea-I-tea}]PF_6$, $[\text{dipa-Ag-dipa}]PF_6$, and $[\text{dipa-I-dipa}]PF_6$ complexes in CD_3CN , and were also characterized by 1H and $^1H-^{15}N$ HMBC NMR spectroscopy.

The 1H NMR spectra of the **1a–6a** silver(I) complexes reveal only single species, but these spectra are virtually identical to the corresponding spectra of free ligands **1–6**. The largest chemical shift change was measured to be 0.08 ppm deshielded for **4a** and **6a**. The 1H NMR spectra of the solutions **4a** and **6a**, obtained by mixing 2.0 equiv. of amine with 1.0 equiv. of $AgPF_6$ in CD_3CN , or from dissolved single crystals of **4a** and **6a**, are equivalent (Figures 4, S5, S7). When **tea** is complexed with silver(I) in CD_3CN , a deshielded chemical shift of 0.12–0.14 ppm are observed (Figure S8). However, upon complexation of **dipa** to $[\text{dipa-Ag-dipa}]PF_6$ in CD_3CN the corresponding 1H NMR spectra of **dipa** itself were almost identical (Figure S9).^[43]

Contrary to 1H NMR chemical shift changes of the silver(I) complexes, those of the iodine(I) complexes **1b–6b** show larger chemical shift changes from those of the free ligands (Figures 4 and S2–S7). The $-CH_2-$ and $-CH_3$ groups closest to the sp^3 -nitrogen atoms are the most affected, being 0.28–0.80 ppm deshielded in comparison to free ligands, the largest shift of 0.80 ppm being observed for the $-CH_2-$ (2,5-dimethylbenzyl) in **4b**. This pattern, including the magnitude of the 1H NMR chemical shift changes and deshielded signal migration, is consistent with the NMR data from $[\text{tea-I-tea}]PF_6$, and $[\text{dipa-I-dipa}]PF_6$, (Figures S8–S9). The aromatic protons, being farther

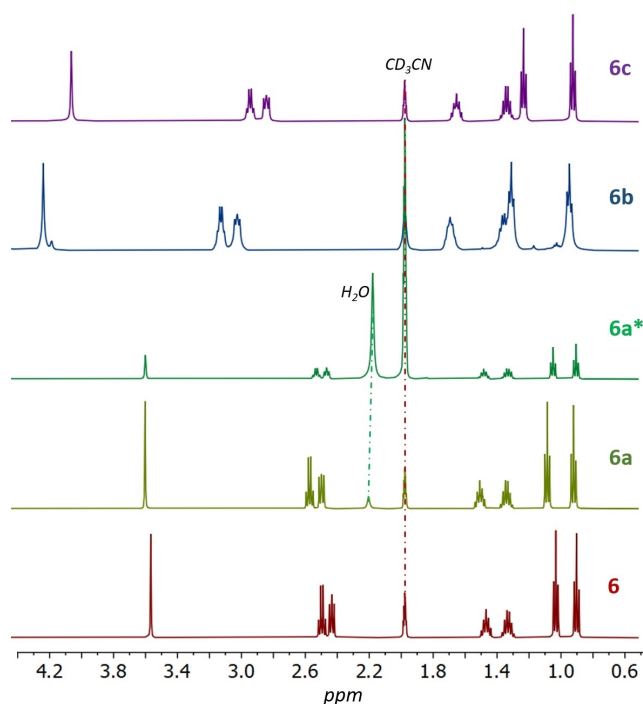


Figure 4. The ^1H NMR spectra of **6–6c**. **6a*** is ^1H NMR spectrum acquired by dissolving single crystals of **6a** in CD_3CN (500 MHz, 298.0 K).

away from the partially positively charged N-atom are the least affected, with a maximum deshielded signal change of 0.22 ppm for **1b**. Comparison of the ^1H NMR spectra of the analogous iodine(I) complexes and their protonated counterparts confirmed the generation of the **1b–6b** iodine(I) complexes, without any additional signals being observed, as shown in Figures 4 and S2–S7. Note that the ^1H NMR spectra of silver(I) and iodine(I) complexes revealed the presence of single species, even when measured from the single crystals of **6a** (Figures 4 and S5) or with a different stoichiometry, viz. 2:1:0.5 equivalents of $6:\text{AgPF}_6:\text{I}_2$ (Figure S11) or 2:1:1 equivalents of $6:\text{AgPF}_6:\text{I}_2$ at temperatures -20°C , -10°C , 0°C , 10°C , 20°C , and 30°C (Figures S12–13). The variable-temperature NMR experiments show that fast ligand exchange^[34] and/or ligand exchange coupled with N-inversion leads to quick equilibration on the NMR time scale.

The ^{15}N NMR chemical shifts provide crucial information about the $[\text{N}–\text{N}]^+$ halogen bond. The ^{15}N NMR data gives characteristic coordination shifts, $\Delta\delta^{15}\text{N}_{\text{coord}}$, depending on whether a $[\text{N}–\text{Ag}–\text{N}]^+$, $[\text{N}–\text{I}–\text{N}]^+$, or $\text{N}^+–\text{H}$ moiety is present.^[21] The $\Delta\delta^{15}\text{N}_{\text{coord}}$ values of silver(I) complexes were all small and did not exceed 6 ppm. No coordination shift was observed upon complexation of **5** to **5a** ($\Delta\delta^{15}\text{N}_{\text{coord}}=0$ ppm), with the largest coordination shift being observed for **6a** ($\Delta\delta^{15}\text{N}_{\text{coord}}=6$ ppm). The $\Delta\delta^{15}\text{N}_{\text{coord}}$ values of the iodine(I) complexes are markedly larger than those of the silver(I) analogs. Only one ^{15}N NMR signal is observed for the silver(I) and iodine(I) complexes, consistent with a single species being present as also observed in the respective ^1H NMR spectra. The $\Delta\delta^{15}\text{N}_{\text{coord}}$ values of the iodine(I) complexes are $\sim 3–5$ times larger than the corresponding values for the silver(I) counterparts, indicating a stronger interaction between the iodine(I) and the coordinating nitrogen atoms of the ligands (Table 1). However the observed $\Delta\delta^{15}\text{N}_{\text{coord}}$ for **1b–6b** are $\sim 70–100$ ppm smaller than those of reported aromatic iodine(I) complexes^[25] and $\sim 6–10$ ppm larger than $[(\text{quinuclidine})_2]^+[\text{22}]$ and $[(1\text{-ethylpiperidine})_2]^+[\text{22}]$ complexes.

In contrast to the reported ^{15}N NMR signals of pyridinic silver(I) and iodine(I) complexes, which exhibit negative ^{15}N NMR chemical shift changes, the silver(I) and iodine(I) amine complexes exhibit positive ^{15}N NMR chemical shift changes (Figure 5a), a trend that is consistent with other sp^3 -nitrogen ligands, viz. $[\text{tea}–\text{I}–\text{tea}]^+$, $[\text{dipa}–\text{I}–\text{dipa}]^+$ (Figures S8 and S9), $[(\text{quinuclidine})_2]^+[\text{22}]$ and $[(1\text{-ethylpiperidine})_2]^+[\text{22}]$. The $\Delta\delta^{15}\text{N}_{\text{coord}}$ values of iodine(I) complexes **1b–6b** and protonated ligands **1c–6c** show the same trend as has been demonstrated for similar pyridinic systems.^[21]

Despite vigorous attempts only the **4a** and **6a** silver(I) complexes formed single crystals and were characterized by X-ray crystallography (Figures 5b and c). Both **4a** and **6a** exclusively crystallize in a centrosymmetric space group, **4a** in $P-1$ and **6a** in $P4/ncc$ as *meso*-complexes, i.e., they have R/S - or S/R -configurations. The complexes **4a** and **6a** are the second examples of linear *bis*-coordinate $[\text{N}–\text{M}–\text{N}]^+$ transition metal complexes from $\text{R}_3\text{R}_2\text{R}_1\text{N}$ tertiary amines. The only previous example is $[\text{bis}(9\text{-}(\text{methylaminomethyl})\text{anthracene})_2\text{Ag}]\text{PF}_6$ ^[19] which is also *meso*-complex (space group monoclinic $C2/c$). The symmetry of the complexes is most likely the reason why these complexes crystallize in the *meso*-form. In contrast to the pure R,R and S,S -enantiomers, the *meso*-complex is more symmetric,

Table 1. The $\Delta\delta^{15}\text{N}_{\text{coord}}$ values of complexes **1a–6a**, **1b–6b**, and salts **1c–6c** in CD_3CN , (298.0 K). The DFT calculated $^+\text{Ag}–\text{N}$ and $^+\text{I}–\text{N}$ bond energies (kJ/mol)^[a] for **1a–6a** and **1b–6b** at the M06-2X/def2-TZVP level of theory in acetonitrile.

Comp	$\Delta\delta^{15}\text{N}$	ΔE_{int}	Comp	$\Delta\delta^{15}\text{N}$	ΔE_{int}	Comp	$\Delta\delta^{15}\text{N}$
1a	3.9	–91.6	1b	15.6	–266.3	1c	15.2
2a	5.2	–82.9	2b	17.3	–269.4	2c	16.6
3a	3.6	–94.1	3b	14.9	–273.7	3c	12.6
4a	4.0	–100.5	4b	19.2	–269.8	4c	15.0
5a	0.1	–79.8	5b	15.5	–259.4	5c	12.4
6a	6.1	–79.8	6b	13.1	–278.6	6c	8.6

[a] Estimated using the free energy of the following transformation: $[\text{L}–\text{X}–\text{L}]^+ \rightarrow 2\text{L} + \text{X}^+$; X = Ag and I.

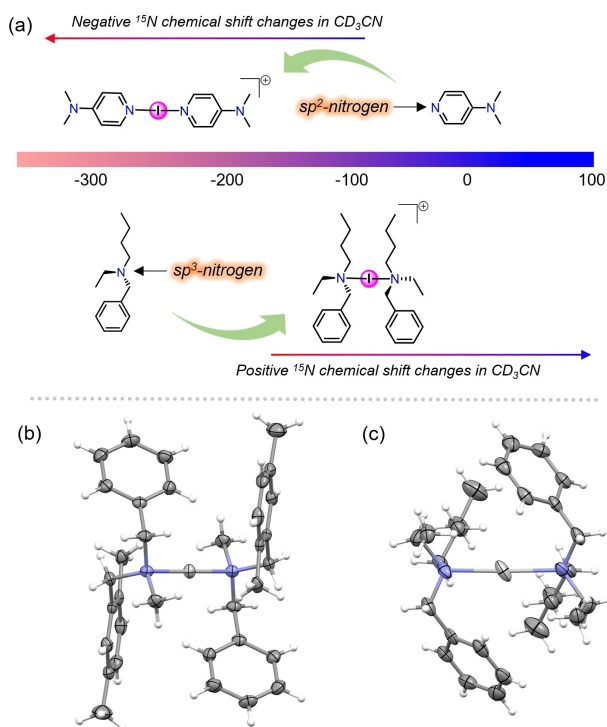


Figure 5. (a) Comparison of the ^{15}N NMR chemical shift changes in **dmap** and aliphatic amines, and their silver(I) and iodine(I) complexes in CD_3CN . Note: The placement of the ligand and their iodine(I) structures on the scale is only for reference. The X-Ray crystal structures of **4a** (b) and **6a** (c) with the thermal displacement parameter at 50% probability level. PF_6^- anions and minor disordered parts in **6a** are omitted for clarity.

making it possible that in the crystal lattice the central silver(I) cation to reside on an inversion center (in all cases the asymmetric unit contains half of the complex). Similar meso-form crystallization has been observed from a 1:1 mixture of chiral *R,R* and *S,S* metal complex.^[44] The Ag–N [**4a**: 2.1927(16) Å; **6a**: 2.191(7) Å] and N...N [**4a**: 4.385 Å; **6a**: 4.336 Å] distances are, as expected, very similar to the pyridine-based $[\text{N}–\text{Ag}–\text{N}]^+$ complexes.^[25] The N–Ag–N geometry of **4a** is linear, whereas **6a** [163.3(4)°] deviates from linearity, possibly due to packing forces. In both **4a** and **6a**, the silver(I) is surrounded by aryl/alkyl groups in a *trans* fashion. In this configuration, the complexes are stabilized through the $\text{Ag}^+ \cdots \pi$ [ca. 2.9–3.2 Å] and $\text{Ag} \cdots \text{H}–\text{C}$ [ca. 2.5–3.1 Å] short contacts. It is important to note that **4a** and **6a** crystal structures do not have solvent molecules, but acetonitrile-silver(I) complexes such as $[(\text{CH}_3\text{CN})_2\text{Ag}]^+$,^[45] $[(\text{CH}_3\text{CN})_3\text{Ag}]^+$,^[46] $[(\text{CH}_3\text{CN})_4\text{Ag}]^+$ ^[47] and $[(\text{CH}_3\text{CN})_n\text{Ag}]^+$ ^[48] could exist in solution, yet only **4a** and **6a** crystallized out from the solution.

In order to access the electron donating power of sp^3 nitrogen in **1–6**, DFT calculations (See ESI for details) were performed to calculate the negative minima electrostatic potential ($V_{s,\text{min}}$) of the nitrogen in **1–6**. The calculations show that the $V_{s,\text{min}}$ values of **1–6** (–69.2 to –123.3 kJ/mol) are less negative than DMAP (–206.3 kJ/mol). In all cases, the combined quantum theory of atoms-in-molecules (QTAIM) and non-covalent interaction (NCI) plot index analysis shows the presence C–H...N van der Waals contacts (Figure S23). In **4**, the

C–H...N interaction is further characterized by a bond critical point (BCP) and a bond path connect the C–H to the nitrogen, evidencing the existence of a hydrogen bond (HB) with a strength of 7.4 kJ/mol that reduces the basicity of the N-atom.

The M06-2X/def2-TZVP^[49] level of theory with acetonitrile PCM solvent model was used to estimate the interaction strengths (ΔE_{int}) of $[\text{N}–\text{Ag}–\text{N}]^+$ coordination bonds and $[\text{N}–\text{I}–\text{N}]^+$ halogen bonds. The ΔE_{int} values of $[\text{N}–\text{I}–\text{N}]^+$ in **1b–6b** are ~170–200 kJ mol^{–1} larger than those of the $[\text{N}–\text{Ag}–\text{N}]^+$ in their corresponding silver complexes **1a–6a**. Correspondingly they are ~100 kJ mol^{–1} larger than that of the *bis*-quinuclidine- and *bis*-1-ethylpiperidine-iodine(I),^[22] and ~40–50 kJ mol^{–1} larger than that of the unrestrained *bis*-pyridine-iodine(I)^[20] complexes, and ~80–100 kJ mol^{–1} larger than of the restrained *bis*[1,2-*bis*(2'-pyridylethynyl)benzene-iodine(I)]^[50] complex. The N–I bond energies of **1b–6b** are greater than 260 kJ mol^{–1}, which can be attributed to an exceptionally large Lewis basicity of the nitrogen of the tertiary amines. It should be noted that the bond rotation energies of the alkyl and aryl substituents, in comparison to the N–I energies (≥ 260 kJ mol^{–1}), are insignificant.

Given the weak stabilizing forces between N-alkyl/aryl groups and the silver(I) that have been observed in the crystal structures, the same alkyl/aryl groups closest to the iodine(I) complexes were investigated by performing a QTAIM/NCI plot analysis on *meso*-**1b** (Figure 6). In addition to several intra-complex C–H... π contacts, BCPs and bond pathways clearly show the presence of $\text{I}^+ \cdots \text{H}–\text{C}$ and $\text{I}^+ \cdots \pi$ contacts between alkyl/aryl groups and the iodine(I) electron belt. This finding explains how the flexible aromatic and C–H groups are drawn to the electron belt of the iodine(I) to form HBs, which may be perturbing the iodine(I) σ -hole intensity. Additionally, it is possible that these $\text{I}/\text{Ag}^+ \cdots \text{H}–\text{C}$ contacts are creating a hydrophobic pocket to preserve the integrity of the Ag–N and I–N bonds.

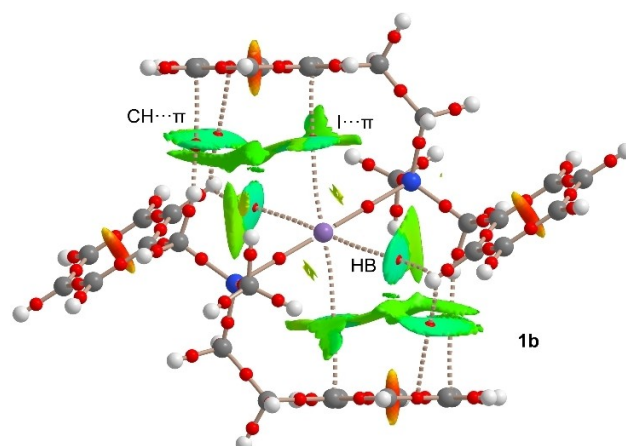


Figure 6. QTAIM/NCI plot analysis of **1b** displaying intra-halonium ion complex $\text{I}^+ \cdots \text{H}–\text{C}$, $\text{I}^+ \cdots \pi$ and $\text{C}–\text{H} \cdots \pi$ short contacts.

Conclusions

In conclusion, the amine ligands coordinate to a silver(I) to produce $[R_3R_2R_1N-Ag-R_1R_2R_3]^+$ complexes, which then undergo the silver(I)→iodine(I) cation exchange reaction. The 1H and ^{15}N NMR studies manifest the formation of single silver(I) and iodine(I) species. The solution very likely contains all possible diastereomers: the *R,R* and *S,S*-enantiomers and the *meso-R,S/S,R*, due to the rapid nitrogen lone pair interconversion of the amine ligands, though only the *meso*-silver(I) complexes could be crystallized out of the mixture. Thus, the observed NMR spectra is interpreted to represent the time-averaged configuration of these species. This observation is supported by temperature-dependent NMR experiments that show that only one set of signals, even at low (0 to $-20^\circ C$) temperatures persists, suggesting fast ligand exchange coupled with N-inversion at the NMR time scale. Our results show that iodine(I) complexes from $R_3R_2R_1N$ can be prepared analogously to the Barluenga-type halogen(I) systems through the silver(I)→iodine(I) cation exchange reaction, which themselves could offer new halogen(I)-based reagents with unexplored potential.

Crystallography data

Deposition Numbers 2270296 (for **4a**) and 2270297 (for **6a**) contain the supplementary crystallographic data for this paper. These data are provided free of charge by the joint Cambridge Crystallographic Data Centre and Fachinformationszentrum Karlsruhe Access Structures service.

Supporting Information

The authors have cited additional references within the Supporting Information (Ref. [51–68]).

Acknowledgements

The authors gratefully acknowledge financial support from the Academy of Finland (RP grant no. 298817, K.R. 351121) and University of Jyväskylä.

Conflict of Interests

The authors declare no conflict of interest.

Data Availability Statement

The data that support the findings of this study are available from the corresponding author upon reasonable request.

Keywords: halogen bonds · meso · tertiary amines · X-ray structure · coordination bonds

- [1] Chirality, In *The IUPAC Compendium of Chemical Terminology*, International Union Of Pure And Applied Chemistry (IUPAC), Research Triangle Park, NC, 2014.
- [2] T. Imamoto, *Proceedings of the Japan Academy, Series B* 2021, 97, 520–542.
- [3] M. Dutartre, J. Bayardon, S. Jugé, *Chem. Soc. Rev.* 2016, 45, 5771–5794.
- [4] S. Otocka, M. Kwiatkowska, L. Madalińska, P. Kielbasiński, *Chem. Rev.* 2017, 117, 4147–4181.
- [5] J. D. Morrison, *Asymmetric Synthesis*, Vol 5, Academic Press, London, Elsevier 2012.
- [6] Pyramidal Inversion, In *The IUPAC Compendium of Chemical Terminology*, International Union Of Pure And Applied Chemistry (IUPAC), Research Triangle Park, NC, 2014.
- [7] J. D. Firth, S. J. Canipa, L. Ferris, P. O'Brien, *Angew. Chem. Int. Ed.* 2018, 57, 223–226.
- [8] M. P. Walsh, J. M. Phelps, M. E. Lennon, D. S. Yufit, M. O. Kitching, *Nature* 2021, 597, 70–76.
- [9] A. R. Katritzky, C. A. Ramsden, J. A. Joule, V. V. Zhdankin, 3rd Edition, *Handbook of Heterocyclic Chemistry*, Elsevier, Oxford, 2010.
- [10] G. S. Denisov, V. A. Gindin, N. S. Golubev, A. I. Koltsov, S. N. Smirnov, M. Rospenk, A. Koll, L. Sobczyk, *Magn. Reson. Chem.* 1993, 31, 1034–1037.
- [11] L. Degennaro, L. Pisano, G. Parisi, R. Mansueto, G. J. Clarkson, M. Shipman, R. Luisi, *J. Org. Chem.* 2015, 80, 6411–6418.
- [12] M. C. De Ceglie, L. Degennaro, A. Falcicchio, R. Luisi, *Tetrahedron* 2011, 67, 9382–9388.
- [13] P. Cornago, R. M. Claramunt, L. Bouissane, J. Elguero, *Tetrahedron* 2008, 64, 3667–3673.
- [14] C. T. Hoang, I. Prokes, G. J. Clarkson, M. J. Rowland, J. H. R. Tucker, M. Shipman, T. R. Walsh, *Chem. Commun.* 2013, 49, 2509–2511.
- [15] L. Giordano, C. T. Hoang, M. Shipman, J. H. R. Tucker, T. R. Walsh, *Angew. Chem. Int. Ed.* 2011, 50, 741–744.
- [16] M. W. Davies, M. Shipman, J. H. R. Tucker, T. R. Walsh, *J. Am. Chem. Soc.* 2006, 128, 14260–14261.
- [17] M. A. Dewey, A. M. Arif, J. A. Gladysz, *J. Chem. Soc., Chem. Comm* 1991, 712–714.
- [18] K. A. Pelz, P. S. White, M. R. Gagné, *Organometallics* 2004, 23, 3210–3217.
- [19] F. Spinelli, S. d'Agostino, P. Taddei, C. D. Jones, J. W. Steed, F. Grepioni, *Dalton Trans.* 2018, 47, 5725–5733.
- [20] A.-C. Carlsson, J. Gräfenstein, A. Budnjo, J. L. Laurila, J. Bergquist, A. Karim, R. Kleinmaier, U. Brath, M. Erdélyi, *J. Am. Chem. Soc.* 2012, 134, 5706–5715.
- [21] L. Turunen, M. Erdélyi, *Chem. Soc. Rev.* 2020, 49, 2688–2700.
- [22] J. S. Ward, A. Frontera, K. Rissanen, *Dalton Trans.* 2021, 50, 8297–8301.
- [23] C. Wyganowski, *Pol. J. Chem.* 1978, 52, 203.
- [24] L. Turunen, A. Peuronen, S. Forsblom, E. Kalenius, M. Lahtinen, K. Rissanen, *Chem. Eur. J.* 2017, 23, 11714–11718.
- [25] J. S. Ward, K.-N. Truong, M. Erdélyi, K. Rissanen, in *Comprehensive Inorganic Chemistry III (Third Edition)*, Elsevier, Oxford, 2023, pp. 586–601.
- [26] J. Barluenga, F. González-Bobes, M. C. Murguía, S. R. Ananthoju, J. M. González, *Chem. Eur. J.* 2004, 10, 4206–4213.
- [27] G. Espuña, G. Arsequell, G. Valencia, J. Barluenga, J. M. Alvarez-Gutiérrez, A. Ballesteros, J. M. González, *Angew. Chem. Int. Ed.* 2004, 43, 325–329.
- [28] J. Barluenga, J. M. González, P. J. Campos, G. Asensio, *Angew. Chem. Int. Ed. Engl.* 1985, 24, 319–320.
- [29] E. Taipale, M. Siepmann, K.-N. Truong, K. Rissanen, *Chem. Eur. J.* 2021, 27, 17412–17419.
- [30] J. S. Ward, *CrystEngComm* 2022, 24, 7029–7033.
- [31] S. B. Hakkert, M. Erdélyi, *J. Phys. Org. Chem.* 2015, 28, 226–233.
- [32] A.-C. Carlsson, J. Gräfenstein, J. L. Laurila, J. Bergquist, M. Erdélyi, *Chem. Commun.* 2012, 48, 1458–1460.
- [33] J. S. Ward, G. Fiorini, A. Frontera, K. Rissanen, *Chem. Commun.* 2020, 56, 8428–8431.
- [34] S. Yu, J. S. Ward, *Dalton Trans.* 2022, 51, 4668–4674.
- [35] M. Mattila, K. Rissanen, J. S. Ward, *Chem. Commun.* 2023, 59, 4648–4651.
- [36] S. Lindblad, K. Mehmeti, A. X. Veiga, B. Nekouishahraki, J. Gräfenstein, M. Erdélyi, *J. Am. Chem. Soc.* 2018, 140, 13503–13513.
- [37] L. Turunen, U. Warzok, R. Puttreddy, N. K. Beyeh, C. A. Schalley, K. Rissanen, *Angew. Chem. Int. Ed.* 2016, 55, 14033–14036.

- [38] L. Turunen, U. Warzok, C. A. Schalley, K. Rissanen, *Chem* **2017**, *3*, 861–869.
- [39] E. Taipale, J. S. Ward, G. Fiorini, D. L. Stares, C. A. Schalley, K. Rissanen, *Inorg. Chem. Front.* **2022**, *9*, 2231–2239.
- [40] A. Vanderkooy, A. K. Gupta, T. Földes, S. Lindblad, A. Orthaber, I. Pápai, M. Erdélyi, *Angew. Chem. Int. Ed.* **2019**, *58*, 9012–9016.
- [41] G. Gong, S. Lv, J. Han, F. Xie, Q. Li, N. Xia, W. Zeng, Y. Chen, L. Wang, J. Wang, S. Chen, *Angew. Chem. Int. Ed.* **2021**, *60*, 14831–14835.
- [42] H. Fang, K. Xie, S. Kemper, M. Oestreich, *Angew. Chem. Int. Ed.* **2021**, *60*, 8542–8546.
- [43] A.-C. Carlsson, M. Uhrbom, A. Karim, U. Brath, J. Grafenstein, M. Erdélyi, *CrystEngComm* **2013**, *15*, 3087–3092.
- [44] X.-D. Zheng, Y.-L. Huang, Y.-P. Tong, *Inorganica Chim Acta* **2018**, *482*, 454–459.
- [45] M. Raducan, C. Rodríguez-Esrich, X. C. Cambeiro, E. C. Escudero-Adán, M. A. Pericàs, A. M. Echavarren, *Chem. Commun.* **2011**, *47*, 4893–4895.
- [46] P. Thuéry, J. Harrowfield, *CrystEngComm* **2016**, *18*, 1550–1562.
- [47] J. M. Ba, k, Effendy, S. Grabowsky, L. F. Lindoy, J. R. Price, B. W. Skelton, A. H. White, *CrystEngComm* **2013**, *15*, 1125–1138.
- [48] D. V. Peryshkov, S. H. Strauss, *Inorg. Chem.* **2017**, *56*, 4072–4083.
- [49] D. Sethio, G. Raggi, R. Lindh, M. Erdélyi, *J. Chem. Theory Comput.* **2020**, *16*, 7690–7701.
- [50] A. Christin Reiersølmoen, S. Battaglia, S. Øien-Ødegaard, A. Kumar Gupta, A. Fiksdahl, R. Lindh, M. Erdélyi, *Chem. Sci.* **2020**, *11*, 7979–7990.

Manuscript received: July 7, 2023

Accepted manuscript online: September 8, 2023

Version of record online: October 26, 2023